Quantum Theory Atoms in Molecules Charge−Charge Flux−Dipole Flux Models for the Infrared Intensities of Benzene and Hexafluorobenzene

João Viçozo da Silva, Jr.,[†] Anselmo E. Oliveira,[‡] Yoshiyuki Hase,[†] and Roy E. Bruns*,[†]

Instituto de Química, Universidade Estadual de Campinas, CP 6154, 13084-970 Campinas, SP, Brazil, and Instituto de Quimica, Universidade Federal de Goiás, CP 131, 74001-970 Goiânia, GO, Brazil

Received: April 8, 2009; Revised Manuscript Received: May 15, 2009

The infrared fundamental intensities of benzene and hexafluorobenzene have been calculated at the MP2/6-311++G(3d,3p) level. The theoretical values are in excellent agreement with the averaged experimental C_6H_6 results having a rms error of 15.3 km mol^{-1}. However, the theory badly underestimates the CF stretching and ring deformation intensities of C_6F_6 having an overall rms error of 141 km mol^{-1}. The theoretical results confirm the dipole moment derivative signs previously attributed on the basis of the comparison of C_6H_6 and C_6D_6 derivatives and semiempirical molecular orbital results. A quantum theory atoms in molecules charge−charge flux−dipole flux interpretation of the theoretical results shows that electronic density changes for out-of-plane vibrations can be explained using a simple bond moment−rehybridization moment model proposed many years ago. However, these changes were found to be much more complicated for the in-plane vibrations involving important charge flux and dipole flux contributions for both molecules as well as contributions from the displacement of equilibrium atomic charges for hexafluorobenzene.

Introduction

The infrared fundamental intensities of benzene and hexafluorobenzene were measured in the gas phase some years ago by several research groups.[1−9] Interest originally centered on the interpretation of the infrared intensity parameters in terms of CH and CF bond moments as well as on an electron rehybridization moment of the ring π electrons. Out-of-plane deformations were expected to be strongly affected by rehybridization moments, whereas in-plane deformations were not. This simple bond dipole−rehybridization moment model was found to describe the intensity differences in the in-plane and out-of-plane CH and CF deformations adequately.[2,8] Later, however, semiempirical CNDO results suggested essentially equal rehybridization moments for the in-plane and out-of-plane CH deformations of benzene.[10] These findings were confirmed by a charge−charge flux−overlap model analysis of density functional results for benzene.[11]

Recently, our group has proposed the application of the charge−charge flux−dipole flux model using atomic charges and dipoles obtained from the quantum theory atoms in molecules (QTAIM/CCFDF)[12−14] for interpreting the infrared fundamental intensities of molecules. The model is based on the atoms in molecules theory proposed by Bader and collaborators[15,16] and has been applied to the molecular vibrations of diatomic and polyatomic molecules including the fluoro-, chloro-, and fluorochloromethanes[14] as well as the difluoro- and dichloroethylenes.[17] It can describe the electronic changes that accompany molecular vibrations by movements of equilibrium atomic charges, intramolecular charge transfer, and changes in the atomic dipoles. The dipole changes can be interpreted to be changes in the polarization of the electron density. If the bond moment−rehybridization moment model holds for the out-of-plane benzene and hexafluorobenzene vibrations, then one can expect null intramolecular charge transfer contributions, whereas movements of static atomic charges and changes in the atomic dipoles should be important. However, all three contributions could be significant for the in-plane CH and CF deformations. Furthermore, the CCFDF model partitions the charge and dipole fluxes into atomic contributions. In this way, the rehybridization moments are directly expressed by the dipole flux terms of the carbon atoms and can be calculated in a straightforward way.

Atomic charges and atomic dipoles obtained from other methods might be used in a CCFDF model. Besides QTAIM, ChelpG atomic charges and dipoles are readily accessible and have been shown to be capable of reproducing the infrared intensities of the fluorochloromethanes adequately.[18] However, only the QTAIM charge and dipole values were consistent with electronegativity and chemical valency concepts. As such, the QTAIM parameters have been used in this application.

Polar tensor[19,20] values calculated from the experimental intensities of C_6H_6 and C_6F_6 were first reported more than 30 years ago. The elimination of the sign ambiguities for the dipole moment derivatives of C_6H_6 was first attempted by comparison with derivatives from the intensity results for the isotopically related molecules, C_6H_5D and *p*-$C_6H_4D_2$.[1] Later, these preferred sign choices for the dipole moment derivatives were confirmed by a comparison of the C_6H_6 polar tensor element values with those obtained for C_6D_6 using the isotopic invariance criterion and semiempirical molecular orbital calculations.[20] Because the quantum chemical derivative estimates were essential for choosing the correct sets of polar tensors for these molecules, the sign ambiguity problems for benzene and hexafluorobenzene are re-examined here using more reliable theoretical procedures. First of all, ab initio molecular orbital results at the MP2/6-311++G(3d,3p) level are used to provide additional information for the benzene and hexafluorobenzene sign selections. The experimental force field for benzene was recalculated to validate the normal coordinates used in this work to transform the experimental gas-phase intensities into dipole moment derivative

* Corresponding author. E-mail: bruns@iqm.unicamp.br.
[†] Universidade Estadual de Campinas.
[‡] Universidade Federal de Goiás.

10.1021/jp903255e CCC: $40.75
Published on Web 06/12/2009

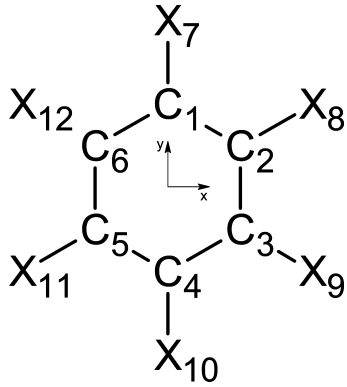

Figure 1. Equilibrium atomic positions and atom numbering scheme.

and polar tensor values. Then, the experimentally derived polar tensor elements are compared with those obtained from quantum chemical calculations and the QTAIM/CCFDF model. The charge, charge flux, and dipole flux contributions of each atom are examined to determine whether the bond moment−rehybridization moment model is supported at the quantum theoretical level for all C_6H_6 and C_6F_6 vibrations.

Calculations

The C_6H_6 polar tensors have been previously determined exclusively from experimental data.[21] Gas-phase fundamental infrared intensities were taken from Overend for C_6H_6[1] and Dows and Pratt for C_6D_6,[4] and the normal coordinate transformation matrices were taken from Duinker and Mills[22] for C_6H_6 and Albrecht[23] for C_6D_6. For C_6F_6 the experimental infrared intensities and normal coordinates were from Steele and Wheatley[8] and Person and collaborators.[9] Experimental internuclear distances were used for calculations involving the experimental intensities.[24,25] The equilibrium atomic positions and atom numbering scheme are shown for the space-fixed Cartesian coordinate system[2] in Figure 1. Alternative normal coordinate transformations were calculated by least-squares fits of the vibrational secular equations to the observed frequencies (corrected for anharmonicity) of C_6H_6, C_6D_6, and $^{13}C_6H_6$ as well as of C_6F_6 using the NTC6 normal coordinate treatment package.[26] These normal coordinates are in excellent agreement with those that had been used in the earlier polar tensor calculations.[21]

Molecular orbital calculations of polar tensors, dipole moment derivatives, and fundamental intensities were carried out with the Gaussian03[27] computer program on Opteron (875) processors in our laboratory. Theoretical equilibrium geometries were used in all quantum chemical polar tensor calculations. Møller−Plesset frozen-core perturbation theory was used with a 6-311++G(3d,3p) basis set. Atomic charges and dipoles were obtained from the relaxed densities of the frozen-core MP2 energies of the Gaussian program using the DENSITY=CURRENT option and the MORPHY98[28] program. The fluxes were calculated numerically from ±0.05 Å atomic Cartesian distortions. Charge, charge flux, and dipole flux contributions to the dipole moment derivatives were calculated using the PLACZEK program.[29]

Results

The experimental infrared intensities for C_6H_6 and C_6F_6 are compared with the theoretical values in Table 1. The MP2/6-311++G(3d,3p) intensity values of benzene are in very good agreement with the averaged experimental values having root-mean-square (rms) errors of 15.3 km mol^{-1}. However, the rms error between the MP2 results and the experimental intensities of C_6F_6 is much larger, 141 km mol^{-1}, with the theory overestimating the CF stretching intensity and the ring deformation. Similar discrepancies were found for the intensities of CF stretching vibrations in the difluoroethylenes[17] and the F_2CO and F_2CS molecules.[30] However the other C_6F_6 intensities are adequately reproduced by the theory. This can be seen in Figure 2, where the MP2/6-311G++(3d,3p) intensity values are plotted against the experimental values. The QTAIM/CCFDF parameters also result in intensity values that are in excellent agreement with the intensities calculated directly from the MP2/6-311++G(3d,3p) electronic density, as can also be seen in Table 1 and Figure 2. The small differences between the intensities calculated directly from the MP2 electron density and from the QTAIM/CCFDF parameters are due to integration errors in determining the atomic charges and atomic dipoles. As such, both theoretical estimates can be expected to provide reasonably accurate descriptions of the electronic density

TABLE 1: Fundamental Infrared Intensities for C_6H_6, C_6D_6, $^{13}C_6H_6$, and C_6F_6 Measured in the Gas Phase and Calculated from MP2/6-311G++(3d,3p) Wave Functions (km mol^{-1})

molecule	A_{11}[a]	A_{18}	A_{19}	A_{20}
C_6H_6	88.16[b]	8.84	14.86	60.06
	84.60 ± 2.02[c]	8.48 ± 0.09	16.09 ± 0.22	68.68 ± 1.23
		8.82 ± 0.44[d]	13.00 ± 0.65	
		7.48 ± 0.15[e]	13.2 ± 1.2	
average	86.38	8.40	14.29	64.37
MP2	114.2	10.0	11.6	51.9
MP2/QTAIM/CCFDF	106.3	7.6	7.2	55.4
$^{13}C_6H_6$	74.6 ± 3.0	6.52 ± 0.15[e]	12.60 ± 0.20[e]	55.6 ± 1[e]
C_6D_6	49.8 ± 2.5[f]	8.02 ± 0.40	2.90 ± 0.15	35.3 ± 3.0
		8.38 ± 0.15[g]	2.85 ± 0.14	33.70 ± 1.69
average	49.8	8.20	2.88	34.5
C_6F_6	2.60[h]	2.50	546 ± 40	408 ± 30
	4.5 ± 0.8[i]	1.55 ± 0.12		415 ± 50
average	3.6	2.03	546	412
MP2	4.9	2.9	690.1	489.8
MP2/QTAIM/CCFDF	6.0	2.7	724.0	511.8

[a] C_6H_6: ν_{11} = 673 cm^{-1}, out-of-plane CH bend; ν_{18} = 1038 cm^{-1}, in-plane CH bend; ν_{19} = 1486 cm^{-1}, ring deformation; ν_{20} = 3080 cm^{-1}, CH stretch. C_6F_6: ν_{11} = 215 cm^{-1}, out-of-plane CF bend; ν_{18} = 317 cm^{-1}, in-plane CF bend; ν_{19} = 1531 cm^{-1}, ring deformation; ν_{20} = 1020−1002 cm^{-1}, CF stretch. [b] Ref 2, as quoted in ref 1. [c] Ref 1. [d] Ref 3. [e] Ref 5. [f] Ref 4, as quoted in ref 5. [g] Ref 3, as quoted in ref 5. [h] Refs 6 and 8. [i] Ref 9.

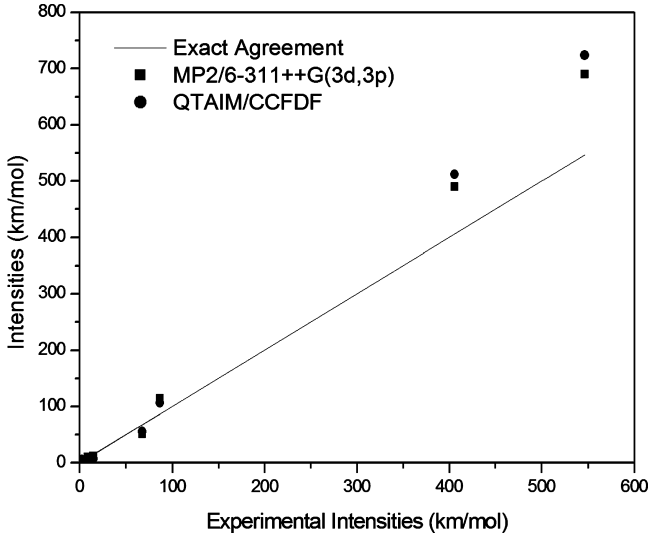

Figure 2. Comparison of the infrared intensities calculated from the MP2/6-311++G(3d,3p) electron density and QTAIM/CCFDF parameters with the experimental intensities.

changes that occur for the normal vibrations of C_6H_6 and C_6F_6, except for possibly the CF stretch and C_6F_6 ring deformation.

The polar tensor elements for all $\partial p/\partial Q_i$ sign combinations of the C_6H_6 and C_6D_6 molecules taken from ref 21 are listed in Table 2. The p_{xx} and p_{yy} values depend on the signs of the $\partial p/\partial Q_i$ of the E_{1u} symmetry species, whereas the sign of p_{zz} depends exclusively on the sign of the A_{2u} derivative. The theoretical values of these elements obtained at the MP2/6-311++G(3d,3p) level are included in this table. The correct signs for the out-of-plane derivatives for the coordinate system in Figure 1 can be obtained from the comparison of the experimental alternatives with the MP2/6-311++G(3d,3p) values. The out-of-plane $p_{zz}^{(C_1)}$ value of −0.116 e and $p_{zz}^{(H_7)}$ value of +0.116 e are preferred because they are very close to the corresponding theoretical values, −0.14 e and +0.14 e, respectively.

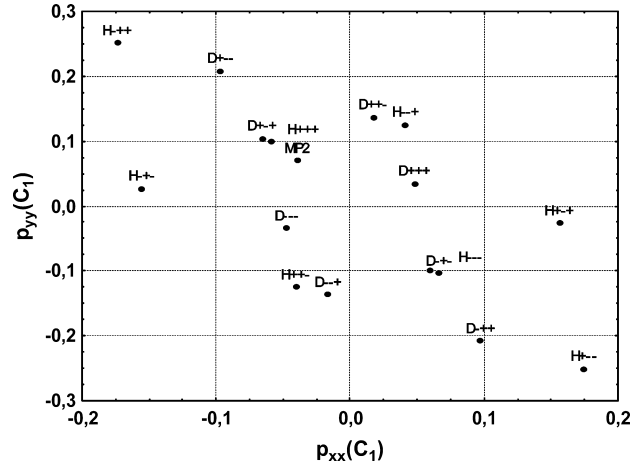

Figure 3. Graph of alternative in-plane polar tensor element values for the possible sign attributions of the $\partial\vec{p}/\partial Q_i$ of C_6H_6 and C_6D_6. (H = C_6H_6, D = C_6D_6).

There are eight sets of in-plane elements for both C_6H_6 and C_6D_6, complicating the selection of the correct set of values. Values for the correct $\partial\vec{p}/\partial Q_i$ sign alternatives can be determined by examining Figure 3, where the $p_{yy}^{(C_1)}$ elements are plotted against the $p_{xx}^{(C_1)}$ elements for the experimental alternative sets of signs. The polar tensor elements should be invariant to isotopic substitution. The H(+ + +)−D(+ − +) and H(− − −)−D(− + −) pairs are in closest proximity to one another, whereas the H(+ + −)−D(− − +) and H(− − +)−D(+ + −) pairs are a bit more separated. An analogous graph of $p_{xx}^{(H_7)}$ versus $p_{yy}^{(H_7)}$ shows the same general pattern. Both the H(+ + +)−D(+ − +) and H(− − −)−D(− + −) isotopic pairs have identical rms differences of 0.0052 e, whereas the other two have rms differences of 0.0141 e. On the basis of the estimated experimental errors[21] in the polar tensor elements, one can expect a difference of 0.011 e if the isotopically invariant criterion holds. This argument favors the H(+ + +)−D(+ − +) and H(− − −)−D(− + −) pairs over the others, although rejection

TABLE 2: Atomic Polar Tensor Element Values for the Carbon, Hydrogen, and Fluorine Atoms As a Function of the Signs of the $\partial p/\partial Q_i$ Determined from Experimental Infrared Intensities and Normal Coordinates

signs of the $\partial p_o/\partial Q_i$	C_6H_6					
A_{2u} E_{1u}	$p_{xx}^{(C_1)}$	$p_{yy}^{(C_1)}$	$p_{zz}^{(C_1)}$	$p_{xx}^{(H_7)}$	$p_{yy}^{(H_7)}$	$p_{zz}^{(H_7)}$
(±)(± ± ±)[a,b]	∓0.059	±0.099	∓0.116	±0.064	∓0.104	±0.116
(±)(± ± ∓)	∓0.041	∓0.125	∓0.116	±0.062	±0.104	±0.116
(±)(± ∓ ±)	±0.156	∓0.027	∓0.116	∓0.011	∓0.118	±0.116
(±)(∓ ± ±)	∓0.174	±0.251	∓0.116	±0.013	∓0.090	±0.116
signs of the $\partial p_o/\partial Q_i$	C_6D_6					
A_{2u} E_{1u}	$p_{xx}^{(C_1)}$	$p_{yy}^{(C_1)}$	$p_{zz}^{(C_1)}$	$p_{xx}^{(D_7)}$	$p_{yy}^{(D_7)}$	$p_{zz}^{(D_7)}$
(±)(± ± ±)	±0.048	±0.034	∓0.121	±0.037	∓0.118	±0.121
(±)(± ± ∓)	±0.017	±0.137	∓0.121	∓0.056	∓0.098	±0.121
(±)(± ∓ ±)[b]	∓0.066	±0.104	∓0.121	±0.061	∓0.099	±0.121
(±)(∓ ± ±)	±0.097	∓0.208	∓0.121	±0.032	±0.078	±0.121
theoretical[d]	−0.048	0.079	−0.134	0.060	−0.091	0.135
signs of the $\partial p_o/\partial Q_i$	C_6F_6[c]					
A_{2u} E_{1u}	$p_{xx}^{(C_1)}$	$p_{yy}^{(C_1)}$	$p_{zz}^{(C_1)}$	$p_{xx}^{(F_7)}$	$p_{yy}^{(F_7)}$	$p_{zz}^{(F_7)}$
(±)(± ± ±)	∓1.210	±0.650	∓0.057	±0.289	±0.271	±0.057
(±)(± ± ∓)	±0.138	±1.018	∓0.057	±0.045	∓1.200	±0.057
(±)(± ∓ ±)[c]	∓0.164	∓1.063	∓0.057	±0.104	±1.124	±0.057
(±)(∓ ± ±)	∓1.184	±0.695	∓0.057	±0.141	±0.348	±0.057
theoretical[d]	0.066	1.251	0.079	−0.162	−1.154	−0.079

[a] Experimental values for the different sign alternatives are from ref 20. [b] (+)(+ + +) for C_6H_6 and (+)(+ − +) for C_6D_6 are the preferred sign combinations. [c] Theoretical values calculated at the MP2/6-31++G(3d,3p) level. [d] (−)(− + −) are the preferred signs for C_6F_6.

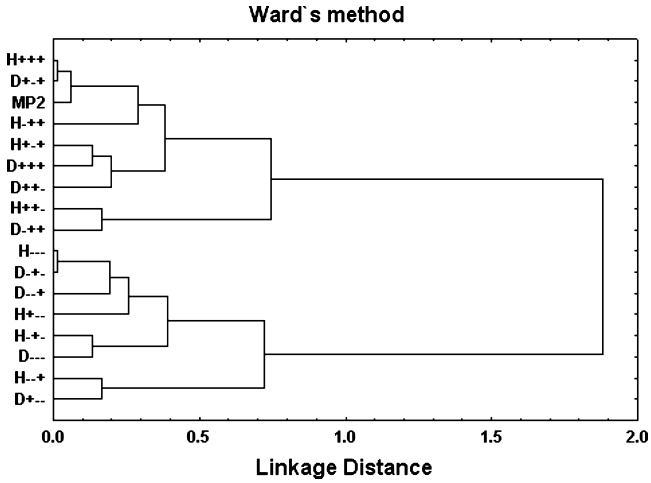

Figure 4. Dendrogram obtained using Ward's method. The preferred H(+ + +) (C_6H_6) and D(+ − +)(C_6D_6) sign sets are in the same cluster with the values calculated at the MP2/6-311++G(3d,3p) level.

of the other two pairs cannot be made at a very high confidence level. However, the quantum chemical estimates at the MP2/6-311++G(3d,3p) level of these polar tensor elements, corresponding to the coordinate system in Figure 1, are in excellent agreement with only the H(+ + +)−D(+ − +) pair, as can be seen in Figure 3. The average tensor elements for this pair have an rms difference of only 0.015 e with the quantum estimates. This difference is 0.062 e for the next closest pair, H(− − +)−D(+ + −). As such, one can conclude that the H(+ + +)−D(+ − +) pair is clearly preferred relative to the alternative E_{1u} sets.

These observations can be confirmed by examining a 4D space with the $p_{xx}^{(C_1)}$, $p_{yy}^{(C_1)}$, $p_{xx}^{(H_7)}$, and $p_{yy}^{(H_7)}$ quantities defining the axes. A dendrogram determined using Ward's hierarchical clustering method[31] applied to the points in this space is shown in Figure 4 and shows that the two sets of experimental points H(+ + +) and D(+ − +) as well as H(− − −) and D(− + −) form the pairs in closest proximity. Of these two pairs, the theoretical results are clustered with the H(+ + +) and D(+ − +) pair, indicating that their corresponding derivatives have the correct polar tensor values.

The isotopic invariance criterion cannot be applied to the C_6F_6 alternative sign combinations in Table 2, so reliance lies exclusively with the agreement between the experimental alternatives and the theoretical values. All theoretical carbon polar tensor elements are positive, whereas the fluorine elements are all negative. The only experimental alternative with these signs is the (−)(− + −) one. Furthermore, it is the experimental alternative that has the smallest rms error with the theoretical values.

Discussion

The charge, charge flux, and dipole flux contributions to the dipole moment derivatives with respect to the normal coordinates of these molecules are presented in Table 3. For benzene, the charge contributions for all derivatives are negligible, and the intensity and derivative values are determined by the flux contributions. For all cases except the out-of-plane vibration, the charge fluxes and dipole fluxes are of opposite sign, partially canceling one another. This negative correlation between the charge and dipole fluxes has already been found for the vibrations of linear molecules,[12] the fluorochloromethanes,[13] the difluoro- and dichloroethylenes,[17] and the X_2CY molecules.[30]

TABLE 3: Charge, Charge Flux, and Dipole Flux Contributions to the Dipole Moment Derivatives in Terms of Normal Coordinates (e amu$^{-1/2}$)

molecule	charge	charge flux	dipole flux	$\partial\vec{p}/\partial Q_i$, total	$\partial\vec{p}/\partial Q_i$, exptl
		C_6H_6			
A_{11}	0.00	0.00	0.33	0.33	0.30
A_{18}	0.00	0.18	−0.24	−0.06	0.05
A_{19}	0.00	−0.40	0.46	0.06	0.06
A_{20}	0.00	0.92	−1.08	−0.16	0.13
		C_6F_6			
A_{11}	−0.56	0.00	0.48	−0.08	0.05
A_{18}	0.22	0.02	−0.20	0.04	0.05
A_{19}	0.49	0.03	−0.01	0.51	0.33
A_{20}	−0.13	0.22	−0.70	−0.61	0.38

The out-of-plane C_6H_6 fundamental is determined solely by the dipole flux contribution. This is in agreement with predictions made by Spedding and Whiffen[2] and by Steele and Wheatley[8] based on the bond moment−rehybridization moment model. Furthermore, the QTAIM/CCFDF model provides results that are consistent with this simple valency model for the out-of-plane bending vibration of C_6F_6. The charge contribution is of comparable magnitude but of opposite sign to the dipole flux contribution, resulting in a much smaller infrared intensity for the C_6F_6 out-of-plane fundamental than that for the C_6H_6 one. This is equivalent to the cancellation of the CF bond and rehybridization moments predicted by the simpler valency model.

However, the bond moment−rehybridization moment model seems to oversimplify the description of the electronic changes occurring for the in-plane vibrations of these molecules. The relatively high intensities of the hexafluorobenzene in-plane vibrations, A_{19} and A_{20}, compared with those for benzene were attributed to the very polar CF bonds. Rehybridization moments were not expected to be as important for in-plane vibrations as they would be for the out-of-plane vibrations, so the CF bond moment contribution would dominate, resulting in high intensity values.

The QTAIM/CCFDF model at the MP2/6-311G++(3d,3p) level indicates much more complex electronic density changes for these vibrations. The low in-plane benzene intensities are seen to result from very efficient cancellations of the charge flux and dipole flux contributions. The charge flux makes major contributions as electronic charge is transferred among atoms during the vibrations. The dipole flux contributions represent polarizations of the electronic density in directions opposite to those owing to electronic charge transfer. As can be seen in Table 3, these dipole flux contributions for benzene can be larger than those found for the out-of-plane vibrations. For the in-plane CF stretching vibration, Q_{20}, the dipole flux is predominant, whereas the equilibrium charge movement is the only important contribution to the dipole moment change for the ring deformation, Q_{19}, explaining the very large intensities for A_{19} and A_{20}. Equilibrium charge movement and dipole flux contributions cancel each other for the CF bending vibration, which is consistent with the small intensity value for A_{18}.

Electronic density changes during molecular vibrations are most easily understood in terms of Cartesian polar tensor elements rather than dipole moment derivatives with respect to normal coordinates. The diagonal and off-diagonal polar tensor elements are given by

$$\frac{\partial p_r}{\partial r_a} = q_a + \sum_i r_i\left(\frac{\partial q_i}{\partial r_a}\right) + \sum_i \frac{\partial m_{i,r}}{\partial r_a} \quad (1)$$

and

$$\frac{\partial p_s}{\partial r_a} = \sum_i s_i\left(\frac{\partial q_i}{\partial r_a}\right) + \sum_i \frac{\partial m_{i,s}}{\partial r_a} \quad (2)$$

where $r,s = x, y, z$, a refers to the displaced atom, q_a and q_i are atomic charges, and $m_{i,r}$ and $m_{i,s}$ are Cartesian components of the atomic dipole moments. Whereas the diagonal elements contain charge, charge flux, and dipole flux contributions, the off-diagonal elements contain only terms for the fluxes. Furthermore, these contributions can be partitioned into atomic contributions within the QTAIM formalism. This is particularly convenient for analyzing electronic density changes in terms of the simple bond moment−rehybridization moment model.

Electronic density changes for the out-of-plane vibrations can be analyzed using the $p_{zz}^{(H_7)}$ and $p_{zz}^{(F_7)}$ polar tensor elements. Values for these polar tensor elements are given in Table 4. Like $\partial\vec{p}/\partial Q_{11}$ for benzene (Table 3), $p_{zz}^{(H_7)}$ has contributions from only the dipole flux. Also, $p_{zz}^{(F_7)}$ has a charge contribution that is 1.17 times larger than and of opposite sign compared with the dipole flux contribution, as does $\partial\vec{p}/\partial Q_{11}$ for C_6F_6.

The QTAIM/CCFDF results for the polar tensor elements given in Table 4 can be decomposed into the individual atomic contributions within the summation terms of Equation 1. For the out-of-plane deformation

$$p_{zz}^{(H_7)} = \frac{\partial p_z}{\partial z_{H_7}} = \frac{\partial m_{C_1,z}}{\partial z_{H_7}} + \frac{\partial m_{H_7,z}}{\partial z_{H_7}} + ... = 0.23\ e - 0.04\ e + ... = 0.13\ e \quad (3)$$

and

$$p_{zz}^{(F_7)} = \frac{\partial p_z}{\partial z_{F_7}} = q_{F_7} + \frac{\partial m_{C_1,z}}{\partial z_{F_7}} + \frac{\partial m_{F_7,z}}{\partial z_{F_7}} + ... = -0.62\ e + 0.42\ e + 0.14\ e + ... = -0.06\ e \quad (4)$$

Only terms with absolute values larger than 0.03 e have been explicitly included in the above equations. The $p_{zz}^{(H_7)}$ element is determined by the $\partial m_{C_1,z}/\partial z_{H_7}$element, 0.23 e. The positive sign corresponds to polarization of the electron density of the C_1 atom in the negative z direction as the H_7 atom moves in the opposite direction. Because the hydrogen atom in benzene has an atomic charge that is close to zero, the out-of-plane dipole moment derivative is determined mostly by atomic dipole moment changes on the neighboring carbon atom. The smaller terms contributing to $p_{zz}^{(H_7)}$ represent small changes in polarizations of electronic densities on the nearest neighboring carbon atoms and on the hydrogen atom displaced in the positive direction. For the deformation where all hydrogen atoms are displaced out-of-plane, only the carbon atomic charge polarizations in the opposite direction to the hydrogen displacements will dominate contributions to $\partial\vec{p}/\partial Q_{11}$ and the A_{11} fundamental intensity.

The $p_{zz}^{(F_7)}$ element has three important contributions owing to the movement of the equilibrium fluorine atomic charge out of the molecular plane, −0.62 e, and the change in the neighboring C_1 atomic dipole that occurs in the opposite direction to the fluorine displacement, +0.42 e, which is reinforced by a change in the atomic dipole of the displaced fluorine atom, +0.14 e. Both atomic dipole contributions cancel the charge contribution resulting in a $p_{zz}^{(F_7)}$ polar tensor element that is smaller than the $p_{zz}^{(H_7)}$ element.

TABLE 4: QTAIM Charge, Charge Flux, and Dipole Flux Contributions to Polar Tensor Elements of C_6H_6 and C_6F_6[a]

molecule	charge	charge flux	dipole flux	total
		C_6H_6		
$p_{xx}^{C_1}$	0.00	0.40	−0.44	−0.04
$p_{yy}^{C_1}$	0.00	−0.66	0.73	0.07
$p_{zz}^{C_1}$	0.00	0.00	−0.14	−0.14
$p_{xx}^{H_7}$	0.00	−0.23	0.28	0.05
$p_{yy}^{H_7}$	0.00	0.49	−0.59	−0.10
$p_{zz}^{H_7}$	0.00	0.00	0.13	0.13
		C_6F_6		
$p_{xx}^{C_1}$	0.61	0.29	−0.83	0.07
$p_{yy}^{C_1}$	0.61	−0.30	0.98	1.29
$p_{zz}^{C_1}$	0.61	0.00	−0.53	0.08
$p_{xx}^{F_7}$	−0.62	−0.06	0.54	−0.14
$p_{yy}^{F_7}$	−0.62	0.14	−0.69	−1.17
$p_{zz}^{F_7}$	−0.62	0.00	0.53	−0.09

[a] Units of electrons, e.

The bond moment−rehybridization model successfully predicts the leading terms in these equations, $\partial m_{C_1,z}/\partial z_{H_7}$ and $\partial m_{C_1,z}/\partial z_{F_7}$, the rehybridization moments of C_6H_6 and C_6F_6, and q_{F_7}, the large negative fluorine atomic charge that is represented by the bond moment. However, the change in the polarization of the charge on the displaced fluorine atom is also seen to be important in canceling the effect of the movement of equilibrium fluorine charge.

Of the individual contributions from eq 1, the fluorine atomic charge contribution to $p_{xx}^{(F_7)}$ is the most important, whereas the charge contribution to $p_{xx}^{(H_7)}$ is negligible. The other important dipole change contributions for the in-plane C_6H_6 and C_6F_6 bond deformations are analogous, as can be seen in the QTAIM/CCFDF equations below

$$p_{xx}^{(H_7)} = \frac{\partial p_x}{\partial x_{H_7}} = \frac{\partial m_{C_1,x}}{\partial x_{H_7}} + \frac{\partial m_{H_7,x}}{\partial x_{H_7}} + \frac{\partial m_{C_6,x}}{\partial x_{H_7}} + \frac{\partial m_{C_2,x}}{\partial x_{H_7}} + \frac{\partial q_{C_6}}{\partial x_{H_7}} x_{C_6} + \frac{\partial q_{C_2}}{\partial x_{H_7}} x_{C_2} + ... \quad (5)$$
$$= (0.16 + 0.04 + 0.05 + 0.05 + -0.04 - 0.04 + ...)\ e = 0.05\ e$$

and

$$p_{xx}^{(F_7)} = \frac{\partial p_x}{\partial x_{F_7}} = q_{F_7} + \frac{\partial m_{C_1,x}}{\partial x_{F_7}} + \frac{\partial m_{F_7,x}}{\partial x_{F_7}} + \frac{\partial m_{C_6,x}}{\partial x_{F_7}} + \frac{\partial m_{C_2,x}}{\partial x_{F_7}} ... \quad (6)$$
$$= (-0.62 + 0.27 + 0.23 + 0.04 + 0.04 + ...)\ e = -0.14\ e$$

The polar tensor element corresponding to the CH in-plane bending deformations has its dominating contribution owing to

changes in the atomic dipole of the carbon atom attached to the dislocated hydrogen atom. However, $p_{xx}^{(F_7)}$ has a dominating negative charge contribution as well as important contributions from atomic dipole changes on the displaced fluorine atom and the carbon atom attached to it. These atomic dipole changes are in the same direction and opposite to the one owing to the movement of equilibrium charge. As such, both $p_{zz}^{(F_7)}$ and $p_{xx}^{(F_7)}$ corresponding to the out-of-plane and in-plane deformations have substantial charge polarizations in opposite directions to the movements of the fluorine atom.

The $p_{yy}^{(H_7)}$ polar tensor element corresponds to the CH stretching vibration and contains important individual charge transfer contributions involving the atoms of the stretched CH bond, that is, the first two terms in eq 7. Also, the third term, involving polarization of the electron density of the carbon atom of this bond, is significant

$$p_{yy}^{(H_7)} = \frac{\partial p_y}{\partial y_{H_7}} = \frac{\partial q_{C_1}}{\partial y_{H_7}} y_{C_1} + \frac{\partial q_{H_7}}{\partial y_{H_7}} y_{H_7} + \frac{\partial m_{C_1,y}}{\partial y_{H_7}} + \ldots = -1.01\,e + 1.46\,e - 0.69\,e + \ldots = -0.10\,e \quad (7)$$

Most of the electronic charge density is transferred from the displaced hydrogen atom to the carbon atom bound to it. As a consequence, polarization of the electronic density on the carbon atom of the bond being stretched is in the same direction as the displaced hydrogen atom, that is, with negative pole in the direction of the stretched hydrogen. Smaller amounts of electronic charge are transferred to other atoms in the molecule.

The individual contributions to the $p_{yy}^{(F_7)}$ element are

$$p_{yy}^{(F_7)} = \frac{\partial p_y}{\partial y_{F_7}} = q_{F_7} + \frac{\partial q_{C_1}}{\partial y_{F_7}} y_{C_1} + \frac{\partial q_{F_7}}{\partial y_{F_7}} y_{F_7} + \frac{\partial m_{C_1,y}}{\partial y_{F_7}} + \frac{\partial m_{F_7,y}}{\partial y_{F_7}} + \frac{\partial q_{C_6}}{\partial y_{F_7}} y_{C_6} + \frac{\partial q_{C_2}}{\partial y_{F_7}} y_{C_2} + \frac{\partial q_{C_4}}{\partial y_{F_7}} y_{C_4} + \frac{\partial q_{F_{12}}}{\partial y_{F_7}} y_{F_{12}} + \frac{\partial q_{F_{10}}}{\partial y_{F_7}} y_{F_{10}} + \frac{\partial q_{F_8}}{\partial y_{F_7}} y_{F_8} + \frac{\partial m_{C_6,y}}{\partial y_{F_7}} + \frac{\partial m_{C_2,y}}{\partial y_{F_7}} + \frac{\partial m_{F_7,y}}{\partial y_{F_7}} + \ldots = (-0.62 - 1.70 + 1.73 - 0.60 - 0.24 + 0.12 + 0.12 - 0.05 + 0.04 - 0.05 + 0.04 + 0.05 + 0.05 + \ldots)\,e = -1.18\,e \quad (8)$$

The four dominating contributions in this equation are analogous to those found for $p_{yy}^{(H_7)}$, except for the large negative charge contribution owing to the displacement of the negative fluorine atom. Electronic charge transfers from the fluorine atom to its neighboring carbon atom on CF stretching. Furthermore, this carbon atom experiences an electronic charge polarization of about the same size and in the same direction as that for $p_{yy}^{(H_7)}$, that is, in the direction of the displaced fluorine atom that has become more positively charged. The dipole flux and charge contributions determine the sense of the dipole moment change for this stretch because the atomic contributions from charge transfer almost cancel one another. The charge transfer for the C_1-F_7 stretch is shown in Figure 5. The carbon bonded to the stretched fluorine receives electron density mostly from that fluorine with smaller amounts from its neighboring carbon atoms.

Conclusions

The dipole moment derivatives of benzene and hexafluorobenzene have been expressed as atomic charge, charge flux, and dipole flux contributions using the QTAIM. The rehybridization moments for these molecules are given by derivatives of the atomic dipoles on the carbon atoms. Although the bond moment−rehybridization moment model is shown to provide an accurate description of electronic density changes for the out-of-plane CH and CF bending vibrations, rehybridization moments are also significant for the in-plane vibrations. The atomic partitioning of charge and dipole fluxes permits an elegant analysis of electronic structure changes during molecular vibrations in terms of classical chemical valency concepts and should be useful in applications on other molecules.

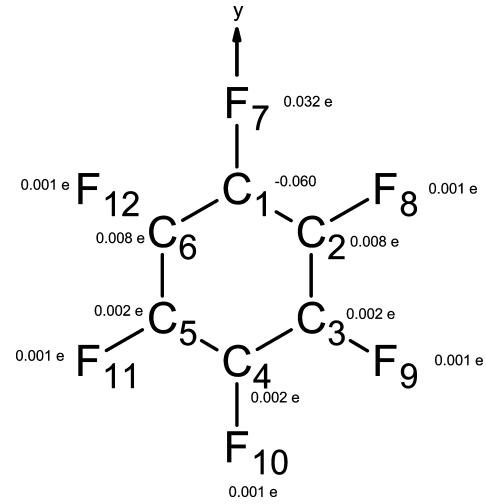

Figure 5. Atomic charge changes on stretching the fluorine atom by 0.05 Å.

Acknowledgment. Financial support from the Fundação de Amparo á Pesquisa do Estado de São Paulo (Fapesp) and the Conselho Nacional de Pesquisa (CNPq) is gratefully acknowledged. J.V.d.S. thanks Fapesp for a doctoral fellowship.

References and Notes

(1) Overend, J. Chapter 10. In *Infrared Spectroscopy and Molecular Structure*; Davies, M., Ed.; Elsevier: Amsterdam, 1963.
(2) Spedding, H.; Whiffen, D. H. *Proc. R. Soc. London, Ser. A* **1956**, *248*, 245.
(3) Ahiyama, M. *J. Mol. Spectrosc.* **1982**, *93*, 154.
(4) Dows, D. A.; Pratt, A. L. *Spectrochim. Acta* **1962**, *18*, 433.
(5) Goodman, L.; Ozkabak, A. G.; Wiberg, K. B. *J. Chem. Phys.* **1989**, *91*, 2069.
(6) Steele, D.; Whiffen, D. H. *J. Chem. Phys.* **1958**, *29*, 1194.
(7) Steele, D.; Wheatley, W. *J. Mol. Spectrosc.* **1969**, *32*, 260.
(8) Steele, D.; Wheatley, W. *J. Mol. Spectrosc.* **1969**, *32*, 265.
(9) Person, W. B.; Olsen, D. A.; Fordemwalt, J. N. *Spectrochim. Acta, Part A* **1966**, *22*, 1733.
(10) Bruns, R. E.; Person, W. B. *J. Chem. Phys. A* **1972**, *57*, 324.
(11) Choi, C. H.; Kertesz, M. *Chem. Phys. Lett.* **1996**, *263*, 697.
(12) Haiduke, R. L. A.; Bruns, R. E. *J. Phys. Chem. A* **2005**, *109*, 2680.
(13) César, P. H.; Faria, S. H. D. M.; Haiduke, R. L. A.; Bruns, R. E.; Vicozo, J. S., Jr. *Chem. Phys.* **2005**, *317*, 35.
(14) Vicozo, J. S., Jr.; Haiduke, R. L. A.; Bruns, R. E. *J. Phys. Chem. A* **2006**, *110*, 4839.
(15) Bader, R. F. W. *Atoms in Molecules: A Quantum Theory*; Clarendon Press: Oxford, U.K., 1990.
(16) Bader, R. F. W.; Larouche, A.; Gatti, C.; Carroll, M. T.; Macdougal, P. J.; Wiberg, K. B. *J. Chem. Phys.* **1987**, *87*, 1142.
(17) Viçozo, J. S., Jr.; Faria, S. H. D. M.; Haiduke, R. L. A.; Bruns, R. E. *J. Phys. Chem. A* **2007**, *111*, 515.
(18) Gomes, T. C. F.; Vicozo, J. S., Jr.; Vidal, L. N.; Vazques, P. A. M.; Bruns, R. E. *Theor. Chem. Acc.* **2008**, *121*, 173.
(19) Person, W. B.; Newton, J. H. *J. Chem. Phys.* **1974**, *61*, 1040.
(20) Morcillo, J.; Biarge, J. F.; Herranz, J. *Ann. R. Soc. Esp. Fis. Quim., Ser. A* **1961**, *57*, 81.
(21) de Barros Neto, B.; Bruns, R. E. *J. Chem. Phys.* **1978**, *68*, 5451.
(22) Duinker, J. C.; Mills, I. M. *Spectrochim. Acta, Part A* **1968**, *24*, 417.

(23) Albrecht, A. C. *J. Mol. Spectrosc.* **1960**, *5*, 236.
(24) Whiffen, D. H. *Philos. Trans. R. Soc. London, Ser. A* **1955**, *248*, 131.
(25) Almeningen, A.; Bastiansen, O.; Seip, R.; Seip, H. M. *Acta Chem. Scand.* **1964**, *18*, 2115.
(26) Hase, Y. *NCT6: A Normal Coordinate Treatment Package*, version 6; Universidade Estadual de Campinas: Campinas, Brazil.
(27) Frisch, M. J.; Trucks, G. W.; Schlegel, H. B.; Scuseria, G. E.; Robb, M. A.; Cheeseman, J. R.; Montgomery J. A., Jr.; Vreven, T.; Kudin, K. N.; Burant, J.C.; Millam, J. M.; Iyengar, S. S.; Tomasi, J.; Barone, V.; Mennucci, B.; Cossi, M.; Scalmani, G.; Rega, N.; Petersson, G. A.; Nakatsuji, H.; Hada, M.; Ehara, M.; Toyota, K.; Fukuda, R.; Hasegawa, J.; Ishida, M.; Nakajima, T.; Honda, Y.; Kitao, O.; Nakai, H.; Klene, M.; Li, X.; Knox, J. E.; Hratchian, H. P.; Cross, J. B.; Bakken, V.; Adamo, C.; Jaramillo, J.; Gomperts, R.; Stratmann, R. E.; Yazyev, O.; Austin, A. J.; Cammi, R.; Pomelli, C.; Ochterski, J. W.; Ayala, P. Y.; Morokuma, K.; Voth, G. A.; Salvador, P.; Dannenberg, J. J.; Zakrzewski, V. G.; Dapprich, S.; Daniels, A. D.; Strain, M. C.; Farkas, O.; Malick, D. K.; Rabuck, A. D.; Raghavachari, K.; Foresman, J. B.; Ortiz, J. V.; Cui, Q.; Baboul, A. G.; Clifford, S.; Cioslowski, J.; Stefanov, B. B.; Liu, G.; Liashenko, A.; Piskorz, P.; Komaromi, I.; Martin, R. L.; Fox, D. J.; Keith, T.; Al.Laham, M. A.; Peng, C. Y.; Nanayakkara, A.; Challacombe, M.; Gill, P. M. W.; Johnson, B.; Chen, W.; Wong, M. W.; Gonzalez, C.; Pople, J. A. *Gaussian 03*; Gaussian, Inc.: Wallingford, CT, 2004.
(28) Popelier, P. L. A. with a contribution from Bone, R. G. A. *MORPHY98*; UMIST: Manchester, U.K., 1998.
(29) Gomes, T. C. F.; Viçozo, J. S., Jr.; Vidal, L. N.; Vazquez, P. A. M.; Bruns, R. E. *Quim. Nova* **2008**, *31*, 1750.
(30) Faria, S. H. D. M.; Viçozo, J. S., Jr.; Haiduke, R. L. A.; Vidal, L. N.; Vazquez, P. A. M.; Bruns, R. E. *J. Phys. Chem. A.* **2007**, *111*, 7870.
(31) Ward, J. H. *J. Am. Stat. Assoc.* **1963**, *58*, 236.

JP903255E